

Fixed points and infrared completion of quantum gravity

N. Christiansen,¹ D. F. Litim,² J. M. Pawłowski,^{1,3} and A. Rodigast¹

¹*Institut für Theoretische Physik, Universität Heidelberg, Philosophenweg 16, 69120 Heidelberg, Germany*

²*Department of Physics and Astronomy, University of Sussex, Brighton, BN1 9QH, U.K.*

³*ExtreMe Matter Institute EMMI, GSI Helmholtzzentrum für Schwerionenforschung mbH, Planckstr. 1, 64291 Darmstadt, Germany*

The phase diagram of four-dimensional Einstein-Hilbert gravity is studied using Wilson’s renormalization group. Smooth trajectories connecting the ultraviolet fixed point at short distances with attractive infrared fixed points at long distances are derived from the non-perturbative graviton propagator. Implications for the asymptotic safety conjecture and further results are discussed.

Introduction. — An important challenge in theoretical physics relates to the quantum nature of gravity and the incorporation of the gravitational force into the successful Standard Model of Particle Physics. A promising avenue is provided through Weinberg’s asymptotic safety conjecture, according to which a quantum theory of metric gravity may very well exist on a fundamental level [1]. The scenario stipulates the existence of an ultraviolet (UV) fixed point which renders the theory finite even beyond the Planck scale, in a manner similar to the well-known weakly-coupled UV fixed point of quantum chromodynamics (QCD). In gravity, and unlike QCD, the fixed point is expected to be interacting and its investigation requires non-perturbative methods. Substantial support in favor of a gravitational UV fixed point has been accumulated in recent years based on continuum studies, see e.g. [2–6] and references therein, lattice simulations [7, 8], and holography [9].

A method of choice in the study of gravity in the continuum is given by Wilson’s renormalization group, based on the infinitesimal integrating-out of momentum degrees of freedom. It permits a systematic analysis even of strongly correlated and strongly coupled theories and offers the prospect for a deeper understanding of gravity in its extremes of shortest and largest distances. Furthermore, insights achieved for other strongly correlated systems such as critical scalar theories and QCD, reviewed in [10, 11], can now be exploited for gravity.

A useful laboratory for quantum gravity is given by the Einstein-Hilbert approximation, which retains Newton’s coupling G_N and the cosmological constant Λ as the relevant couplings. By now, the study of gravitational fixed points within the Einstein-Hilbert theory and the phase diagram has led to a consistent picture with a non-trivial short-distance fixed point in Newton’s coupling and the cosmological constant, see [2, 4–6] and references therein. Infrared fixed points corresponding to a vanishing or negative cosmological constant [12, 13] have been detected as well. For positive cosmological constants, the IR behavior is plagued by additional divergences, though the conjectured existence of an IR fixed point [14] has received some attention recently [12, 13, 15–17].

In this Letter, we derive the fixed points and the

phase diagram of gravity from the RG flow for the non-perturbative graviton propagator. Our derivation of the RG flow differs from previous studies in two main aspects: firstly, we evaluate the flow on flat backgrounds, which permits a better control on how the propagating degrees of freedom drive the RG flow for the relevant couplings. It also provides a consistency check for earlier studies based on background field methods [2–6], bi-metric formulations, [18], and geometric flows [12]. Secondly, we adopt a new bi-local projection technique to identify the scale-dependence of Newton’s coupling and the cosmological constant, offering an improved resolution of the relevant fluctuations in the UV and IR limits of the theory. As a result, we obtain the first global phase diagram with a stable ultraviolet fixed point which connects smoothly with an attractive infrared fixed point at positive cosmological constant.

Gravitational renormalization group. — The present work is done within the functional RG approach which is set up below. It is then utilized for the derivation of the RG flow for Newton’s coupling G_N and the cosmological constant Λ . Under the RG momentum flow, the classical couplings G_N and Λ turn into scale-dependent couplings, whose values depend on the RG scale parameter k . As a function of the latter, the couplings interpolate between the short ($1/k \rightarrow 0$) and long distance regimes ($k \rightarrow 0$) of the theory. It is convenient to introduce the scale dependent, dimensionless couplings $g_N \equiv k^2 G_N / Z_{N,k}$ and $\lambda \equiv \Lambda_k / k^2$, where $Z_{N,k}$ denotes the graviton wavefunction renormalization. In terms of these, the corresponding RG β functions have the form

$$\partial_t g_N = (2 + \eta_N) g_N \quad \text{and} \quad \partial_t \lambda = -2\lambda + \eta_\lambda, \quad (1)$$

with $t \equiv \ln(k/k_0)$ denoting the logarithmic RG ‘time’, and k_0 an arbitrary reference scale. We also introduced the anomalous dimension of the graviton $\eta_N \equiv -\partial_t Z_{N,k} / Z_{N,k}$ and the ‘anomalous dimension’ of the cosmological constant $\eta_\lambda \equiv (\partial_t \Lambda_k) / k^2$. From (1) one can see that the fixed point condition $(\partial_t g_N, \partial_t \lambda) = (0, 0)$ is satisfied if the canonical running due to the mass dimension of G_N and Λ_k is exactly counter-balanced by the running induced by quantum fluctuations. In case of an UV fixed point this scaling is approached in the limit $k \rightarrow \infty$, thus

$$\partial_t \left. \frac{\delta^2 \Gamma_k[\bar{g}; h]}{\delta h^2} \right|_{h=0} = -\frac{1}{2} \left(\text{Diagram 1} + \text{Diagram 2} \right) - 2 \left(\text{Diagram 3} \right) \equiv \text{Flow}^{(2)}$$

FIG. 1: Diagrammatic representation of the flow of the second order vertex function. The dressed graviton propagator is represented by the double line, the ghost propagator by the dashed line, while a dressed vertex is denoted by a dot and the regulator insertion by the crossed circle.

leading to divergence-free couplings at arbitrarily small distances. In order to deduce expressions for η_N and λ we consider the following gauge-fixed effective action,

$$\begin{aligned} \Gamma_k[\bar{g}; h, \bar{C}, C] &= \frac{Z_{N,k}}{16\pi G_N} \int \sqrt{|\bar{g}|} (R(\bar{g}) - 2\Lambda_k) \\ &+ \frac{Z_{\alpha,k}}{2\alpha} \int \sqrt{|\bar{g}|} \bar{g}^{\mu\nu} F_\mu(\bar{g}, h) F_\nu(\bar{g}, h) \\ &- \sqrt{2} \int \sqrt{|\bar{g}|} \bar{C}_\mu M^\mu{}_\nu(\bar{g}, h) C^\nu. \end{aligned} \quad (2)$$

In (2) $R(\bar{g})$ is the Ricci scalar, and the second and third terms are the gauge fixing term and the ghost action. We use the harmonic gauge condition $F_\mu(\bar{g}, h) = \sqrt{2} (\delta_\mu^\beta \bar{\mathcal{D}}^\alpha - \frac{1}{2} \bar{g}^{\alpha\beta} \bar{\mathcal{D}}_\mu) h_{\alpha\beta}$, where $\bar{\mathcal{D}}$ is the covariant derivative with respect to the background connection. The background metric \bar{g} is necessary to construct the gauge fixing and allows for a split $g = \bar{g} + h$ with a fluctuating graviton field h . The background metric comes with its own auxiliary background diffeomorphisms. The effective action is invariant under combined transformations for the background and the fluctuating field [19–23]. The Faddeev-Popov operator reads explicitly $M^\mu{}_\nu = \bar{g}^{\mu\alpha} \bar{\mathcal{D}}^\beta (g_{\alpha\nu} \bar{\mathcal{D}}_\beta + g_{\beta\nu} \bar{\mathcal{D}}_\alpha) - \bar{g}^{\alpha\beta} \bar{\mathcal{D}}^\mu g_{\beta\nu} \bar{\mathcal{D}}_\alpha$. The scale-dependence of $Z_{\alpha,k}$ is irrelevant in Landau-DeWitt gauge, $\alpha = 0$ [12, 20, 23] which we adopt throughout.

We now turn to the scale-dependence of the effective action Γ_k in (2). It is governed by [24],

$$\partial_t \Gamma_k[\bar{g}; \phi] = \frac{1}{2} \text{Tr} \frac{1}{\Gamma_k^{(2)}[\bar{g}; \phi] + \mathcal{R}_k} \partial_t \mathcal{R}_k, \quad (3)$$

where $\phi = (h, \bar{C}, C)$. The Wilsonian regulator \mathcal{R}_k ensures finiteness of the equation, $(\Gamma_k^{(2)} + \mathcal{R}_k)^{-1}$ is the full propagator and $\Gamma_k^{(n)} \equiv \delta^n \Gamma_k / \delta \phi^n$. The trace over the operator product implies a sum over momenta, all internal indices and fields with a minus sign for the ghost fields. We choose a regulator of the form [25–27]

$$\begin{aligned} \mathcal{R}_k(q^2) &= \Gamma_k^{(2)}|_{\lambda=0} r(q^2/k^2) \\ r(z) &= \left(\frac{1}{z} - 1\right) \theta(1-z) \end{aligned} \quad (4)$$

which allows for a largely analytical access. The RG flow (3), (4) together with (2) enables us to compute (1).

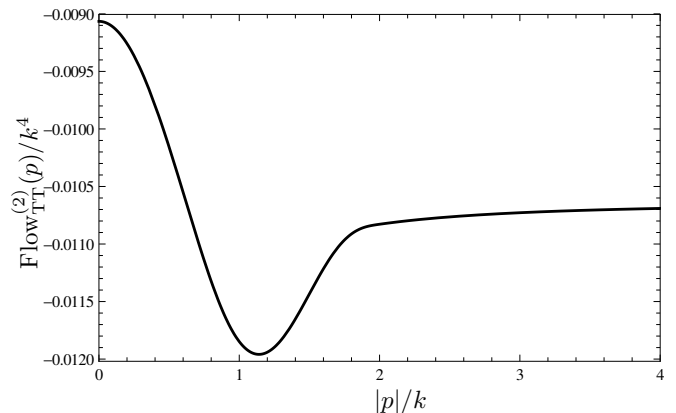


FIG. 2: Dependence of the flow on the external momentum p . In this plot for the parameter values $\lambda = 0$ and $\eta_N = 0$.

Propagator flow and flat backgrounds. — The scale dependence of the effective action Γ_k in (2) is completely governed by that of $\Gamma_k^{(2)}$. It is only left to specify our projection procedure for the flow $\partial_t \Gamma_k^{(2)}$: Firstly we use flat backgrounds $\bar{g}_{\mu\nu} = \delta_{\mu\nu}$. This allows us to distinguish on the right hand side of the flow between propagating modes and the non-dynamical background [23]. This distinction is crucial in Yang–Mills theory to obtain a confining potential of the order-parameter [28]. Moreover, the present setting allows us to study the dependence of $\Gamma_k^{(2)}$ on external momenta p . Following this route, we obtain the flow equation by functional differentiation of (2). It has the diagrammatic representation given in Figure 1. All vertices and propagators are fully dressed. The flow of the inverse propagator contains the three- and the four-point function on the RHS which follow by functional differentiation of (2). The extensive algebra was carried out with the help of FORM and xTENSOR [29, 30]. Note also that the ghosts couple only linearly to the graviton in our approximation.

Einstein-Hilbert gravity. — Next we turn to the definition of the β -functions (1) within the Einstein-Hilbert approximation using an appropriate, bi-local, projection in momentum space. We recall that the relevant information is stored in the dynamical spin two degrees of freedom of the graviton, which is obtained by projecting the flow onto the transverse-traceless (TT) subspace of the symmetric rank-four tensors. Applying this TT projection to the LHS of the flow equation leads to

$$\partial_t \Gamma_{k,\text{TT}}^{(2)} = \frac{1}{32\pi G_N} (p^2 \partial_t Z_{N,k} - 2 \partial_t (Z_{N,k} \Lambda_k)). \quad (5)$$

From an analysis of the momentum structure one infers a quadratic divergence of each diagram in Figure 1, which we have checked explicitly. Hence, one would expect a similar quadratic divergence for large momenta of the right hand side of the TT-flow, denoted with $\text{Flow}_{\text{TT}}^{(2)}(p)$. For large momenta the flow can be calculated analytically

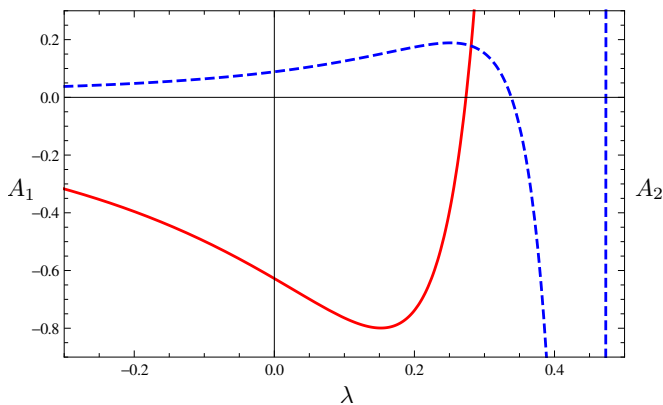


FIG. 3: The functions $A_1(\lambda)$ (solid red line) and $A_2(\lambda)$ (dashed blue line) in the flow of η_N (8). In the limit $\lambda \rightarrow 1/2$ both functions behave as $(1 - 2\lambda)^{-3}$. The function A_2 has a minimal value of -13.6 at $\lambda \approx 0.46$.

and we find a cancellation of all divergent terms, leading to the exact asymptotic behavior

$$\frac{\text{Flow}_{\text{TT}}^{(2)}(p)}{k^4} \xrightarrow{p \rightarrow \infty} \frac{-20 + 42\lambda - 48\lambda^2 + (1 + \lambda)\eta_N}{192\pi^2(1 - 2\lambda)^2}. \quad (6)$$

This general behavior of $\text{Flow}_{\text{TT}}^{(2)}(p)$ is displayed in Figure 2 for $\eta_N = 0$ and $\lambda = 0$.

A similar cancellation has been observed in the context of the Yang–Mills–gravity system where it leads to a vanishing gravitational one-loop contribution to the running of the gauge coupling [23, 31]. To further exploit the structure of the RG flow for $\text{Flow}_{\text{TT}}^{(2)}(p)$ (see Fig. 2), we note that it displays a dip as a function of external momenta p at about $p \approx k$, with a curvature opposite to the one found at $p = 0$. Since fluctuations are integrated out at momenta of the order of the RG scale k , a consistent choice for the evaluation of $\partial_t Z_{N,k}$ is given by the symmetric point $p = k$, which we adopt to identify the RG flow for Newton’s coupling. It also follows from (5) that the cosmological constant appears as a graviton mass defined at vanishing momenta. Therefore, the RG flow for the vacuum energy is deduced from $\partial_t(Z_{N,k}\Lambda_k)$ at $p = 0$. Consequently, we are led to (1) via a bi-local projection in momentum space,

$$\begin{aligned} \partial_t(Z_{N,k}\Lambda_k) &= -16\pi G_N \text{Flow}_{\text{TT}}^{(2)}(p) \Big|_{p=0} \\ \partial_t Z_{N,k} &= 16\pi G_N \partial_p^2 \text{Flow}_{\text{TT}}^{(2)}(p) \Big|_{p=k}. \end{aligned} \quad (7)$$

The virtue of our set-up is that the running of couplings is sensitive to the global (momentum) behavior of the theory as encoded in its two-point function. In addition, the flow of the cosmological constant can be obtained completely analytically. Writing $\eta_\lambda = \eta_N \lambda + g A_3(\lambda, \eta)$,

	g_{N*}^{UV}	λ_*^{UV}	$\lambda_*^{\text{UV}} \times g_{N*}^{\text{UV}}$	θ_1	θ_2
no ghosts	1.95	0.11	0.21	$3.09 + 2.00i$	$3.09 - 2.00i$
with ghosts	2.03	0.22	0.45	8.38	2.60

TABLE I: Fixed point values $(g_{N*}^{\text{UV}}, \lambda_*^{\text{UV}})$, their product, and the critical exponents $\theta_{1,2}$ of the UV fixed point without and with the ghost contributions.

our RG flow (1) takes the final form

$$\begin{aligned} A_3 &= \frac{1 + 4(1 - 2\lambda)^2}{12\pi(1 - 2\lambda)^3} - \eta_N \frac{12 - 45\lambda - 40\lambda^2}{180\pi(1 - 2\lambda)^3} + \frac{1}{\pi}, \\ \eta_N &= \frac{A_1(\lambda)g_N}{1 - A_2(\lambda)g_N} - g_N \frac{237\sqrt{3} - 160\pi}{240\pi^2}. \end{aligned} \quad (8)$$

The last terms originate from the ghosts, and the functions $A_1(\lambda)$ and $A_2(\lambda)$ are known numerically and plotted in the relevant regime in Figure 3.

Fixed points and phase diagram. — The phase diagram of the RG flows (1) with (8) displays four connected fixed points A , B , C and D in the physical regime, see Figure 4. The fixed point A at $(g_{N*}^{\text{UV}}, \lambda_*^{\text{UV}}) \neq (0, 0)$ denotes the asymptotically safe UV fixed point whose coordinates and scaling exponents are given in Tab. I. It is characterised by two UV relevant real eigenvalues, which turn into a complex conjugate pair in the absence of ghost field fluctuations. A complex conjugate pair of eigenvalues, as found in many previous studies, can be lifted via additional interactions e.g. the inclusion of higher derivative interactions. For our set-up, we conclude that the degeneracy in the UV scaling of the Ricci scalar and the vacuum energy is already lifted by the ghost sector. The fixed point B at $(g_{N*}^{\text{IR}}, \lambda_*^{\text{IR}}) = (0, 0)$ is the well-known repulsive Gaussian IR fixed point. It corresponds to classical gravity in the IR with a vanishing cosmological constant. The fixed point D at $(g_{N*}^{\text{IR}}, 1/\lambda_*^{\text{IR}}) = (0, 0^-)$ is IR attractive in both couplings and governs infrared gravity with a negative vacuum energy. In addition we find a non-trivial IR fixed point C at

$$(g_{N*}^{\text{IR}}, \lambda_*^{\text{IR}}) = (0, 1/2), \quad (9)$$

that is connected to the UV fixed point via smooth RG trajectories. It is a distinctive property of the present approach that it admits an infrared completion of quantum gravity for positive cosmological constant. Naively, one would expect classical RG-scaling in the IR fixed point regime [14], for signatures thereof see [17, 26]. Here, we find an asymptotic IR behaviour with non-classical scaling exponents $\Delta_g \approx 5.5$ and $\Delta_{(1-2\lambda)} \approx 1.8$. This IR behavior satisfies the exact scaling relation $\Delta_g = 3\Delta_{(1-2\lambda)}$ within the given numerical accuracy. It implies an asymptotic weakening of gravity, see also [12]. A more detailed analysis will be presented in [32]. In our set-up, the non-classical scaling of the propagator is a consequence of strong IR effects. It will thus be interesting to analyse

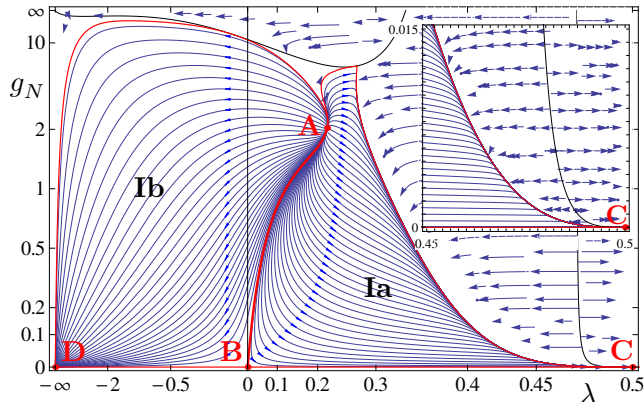


FIG. 4: Fixed points and phase diagram in the (g_N, λ) -plane. Arrows point from the UV to the IR, red lines and points mark separatrices and fixed points, black lines signal a divergence of the flow. The inset magnifies the vicinity of C .

the impact of this scaling on the observable background Newton constant and background cosmological constant, see [12].

It is important to stress that physical short-distance initial conditions in the vicinity of the UV fixed point A leads to trajectories in the regions Ia and Ib. In region Ia all trajectories end into the new IR fixed point C with large anomalous dimensions for the graviton propagator; in region Ib the trajectories end in the IR fixed point D with classical scaling for the graviton propagator. These two regions are separated by the IR instable separatrix leading to the Gaussian FP at B . In turn, all other trajectories terminate in singularities and have no classical regime. Hence, the strong-gravity region is shielded by the separatrices AD ($g_N \leq 33.5$) and AC ($g_N \leq 5.4$) from regions which admit an extended semi-classical regime. The fact that a strong-gravity region is shielded dynamically by the RG flow is also present in previous global UV-IR studies [12, 13], and thus appears to be a generic feature of asymptotically safe gravity.

Summary. — We have studied the phase diagram of quantum gravity with a novel projection technique based on the graviton two-point function. Our study also disentangles the role of fluctuation and background fields, and confirms that gravity becomes asymptotically safe. A further new result are global RG trajectories connecting the short distance fixed point with weak-gravity long distance fixed points. Interestingly, the strong gravity regime is dynamically shielded.

Acknowledgements — This work is supported by the Helmholtz Alliance HA216/EMMI, and by the Science and Technology Facilities Council (STFC) under grant number ST/J000477/1.

- [1] S. Weinberg, General Relativity: An Einstein centenary survey, Eds. Hawking, S.W., Israel, W; Cambridge University Press pp. 790–831 (1979).
- [2] M. Niedermaier and M. Reuter, Living Rev.Rel. **9**, 5 (2006).
- [3] D. F. Litim (2008), 0810.3675.
- [4] A. Codello, R. Percacci, and C. Rahmede, Annals Phys. **324**, 414 (2009), 0805.2909.
- [5] D. F. Litim, Phil.Trans.Roy.Soc.Lond. **A369**, 2759 (2011), 1102.4624.
- [6] M. Reuter and F. Saueressig, New J.Phys. **14**, 055022 (2012), 1202.2274.
- [7] H. W. Hamber, Gen.Rel.Grav. **41**, 817 (2009), 0901.0964.
- [8] J. Ambjorn, A. Goerlich, J. Jurkiewicz, and R. Loll (2012), 1203.3591.
- [9] D. F. Litim, R. Percacci, and L. Rachwal, Phys.Lett. **B710**, 472 (2012), 1109.3062.
- [10] D. F. Litim and D. Zappala, Phys. Rev. **D83**, 085009 (2011), 1009.1948.
- [11] J. M. Pawłowski, AIP Conf.Proc. **1343**, 75 (2011), 1012.5075.
- [12] I. Donkin and J. M. Pawłowski (2012), 1203.4207.
- [13] D. Litim and A. Satz (2012), 1205.4218.
- [14] A. Bonanno and M. Reuter, Phys.Lett. **B527**, 9 (2002), astro-ph/0106468.
- [15] S. Nagy, J. Krizsan, and K. Sailer, JHEP **1207**, 102 (2012), 1203.6564.
- [16] S. Rechenberger and F. Saueressig, Phys.Rev. **D86**, 024018 (2012), 1206.0657.
- [17] C. Contreras and D. F. Litim (2012), in preparation.
- [18] E. Manrique, M. Reuter, and F. Saueressig, Annals Phys. **326**, 463 (2011), 1006.0099.
- [19] D. F. Litim and J. M. Pawłowski, World Sci. pp. 168–185 (1999), hep-th/9901063.
- [20] D. F. Litim and J. M. Pawłowski, Phys. Lett. **B435**, 181 (1998), hep-th/9802064.
- [21] F. Freire, D. F. Litim, and J. M. Pawłowski, Phys. Lett. **B495**, 256 (2000), hep-th/0009110.
- [22] D. F. Litim and J. M. Pawłowski, JHEP **0209**, 049 (2002), hep-th/0203005.
- [23] S. Folkerts, D. F. Litim, and J. M. Pawłowski, Phys.Lett. **B709**, 234 (2012), 1101.5552.
- [24] C. Wetterich, Phys.Lett. **B301**, 90 (1993).
- [25] D. F. Litim, Phys. Rev. **D64**, 105007 (2001), hep-th/0103195.
- [26] D. F. Litim, Phys. Rev. Lett. **92**, 201301 (2004), hep-th/0312114.
- [27] J. M. Pawłowski, Annals Phys. **322**, 2831 (2007), hep-th/0512261.
- [28] J. Braun, H. Gies, and J. M. Pawłowski, Phys.Lett. **B684**, 262 (2010), 0708.2413.
- [29] J. A. M. Vermaseren (2000), arXiv:math-ph/0010025.
- [30] J. Martingarcia, R. Portugal, and L. Manssur, Computer Physics Communications **177**, 640 (2007), 0704.1756.
- [31] D. Ebert, J. Plefka, and A. Rodigast, Phys. Lett. **B660**, 579 (2008), 0710.1002.
- [32] N. Christiansen, J. M. Pawłowski, and A. Rodigast, in preparation (2012).